

JUVENILE SKULLS AND OTHER POSTCRANIAL BONES OF *COELODONTA NIHOWANENSIS* FROM SHANSHENMIAOZUI, NIHEWAN BASIN, CHINA

HAO-WEN TONG^{*1} and XIAO-MIN WANG^{1,2}

¹Key Laboratory of Vertebrate Evolution and Human Origins of Chinese Academy of Sciences, Institute of Vertebrate Paleontology and Paleoanthropology, Chinese Academy of Sciences, Beijing 100044, China, tonghaowen@ivpp.ac.cn;

²University of the Chinese Academy of Sciences, Beijing 100049, China, lishiwangxiaomin@126.com

ABSTRACT—Shanshenmiaozui in the Nihewan Basin of China is the locality that has produced the richest sample of *Coelodonta nihowanensis* material, including a nearly complete juvenile skull and mandible as well as various other cranial, mandibular, and postcranial bones. All of the cranial and mandibular specimens belong to individuals around 1.5 years old. On the basis of both qualitative morphological characters and osteometric measurements, the new specimens can be provisionally referred to the species *Coelodonta nihowanensis*. They also fall within the range of variation seen in late Pleistocene *Coelodonta antiquitatis*, but are distinct from this species in having developed cingula, relatively low-crowned teeth either with or without very thin cement on the surface, vestigial lower incisors, less backward-curved protoloph, and more slender limb bones. The newly discovered juvenile skull of *Coelodonta nihowanensis* from Shanshenmiaozui represents the only known complete juvenile skull of an early member of *Coelodonta*, and therefore has great significance for understanding the development and evolution of the genus. Extensive comparisons with all other *Coelodonta* species, and with extant rhinoceroses, indicate that the new specimens are much more similar to the true woolly rhino *Coelodonta antiquitatis* than to any other taxon.

SUPPLEMENTAL DATA—Supplemental materials are available for this article for free at www.tandfonline.com/UJVP

INTRODUCTION

The woolly rhinoceros is a characteristic Pleistocene animal that was once very widespread throughout the northern part of continental Eurasia and flourished mainly during the late Pleistocene. The rapid evolution and broad distribution of the taxon represent a paleontological mystery, and knowledge about its origins is still very limited.

Until the late 1960s, the true woolly rhino *Coelodonta antiquitatis* (Blumenbach, 1799) was the only species in the genus *Coelodonta* Bronn, 1831. Additional new species and subspecies were subsequently established, which made the taxonomic situation of the woolly rhino clade more complicated. It is now clear that woolly rhinos cannot be used as index fossils for the late Pleistocene, but many uncertainties about these taxa remain. The fact that the genus *Coelodonta* is now known to be non-monospecific raises the question of how *Coelodonta* evolved, and that of when and where *C. antiquitatis* originated.

The fossil record of *Coelodonta* is very rich in China, spanning the entire Pleistocene and even extending back into the Pliocene (Deng et al., 2011). To date, all of the earliest known occurrences of *Coelodonta* are in Chinese strata (Fig. 1). Some of these early specimens have been named as new species (Kahlke, 1969; Chow, 1978; Qiu et al., 2004; Deng et al., 2011) or subspecies (Chia and Wang, 1978; Chow, 1979), but others have been directly referred to the species *C. antiquitatis* (Teilhard de Chardin and Piveteau, 1930; Tang et al., 1983; Li, 1984; Zheng et al., 1985). Because of the poor quality of the early Pleistocene specimens referred to *C.*

antiquitatis, they generally received little attention. Fortunately, some very well preserved fossils of early woolly rhinos have been discovered at the Shanshenmiaozui site in the Nihewan (= Nihewan) Basin in recent years (Tong et al., 2011), which dates to ca. 1.3 Ma. Based on morphological characters and osteometric data, the new specimens can be provisionally placed within the species *C. nihowanensis* Kahlke, 1969. This locality has produced the best early *Coelodonta* fossils ever recovered, and this material has great significance for understanding the evolution of *Coelodonta* and the origin of the true woolly rhino. In this paper, we describe the newly collected *Coelodonta* material from Shanshenmiaozui, and reexamine rhino specimens collected by Teilhard de Chardin from the Nihewan Basin in the 1920s. We also compare the Nihewan material with fossils of *C. antiquitatis* from Sjara-osso-gol.

TERMINOLOGY AND METHODS

Terminology—The terminology applied to tooth crown cusps and loph is well established in the case of the upper teeth, but no similar consensus exists for the lower teeth and particularly for the lophids. The conflicting nomenclatural schemes for the features of the lower teeth were aptly summarized by Qiu and Wang (2007). The terminology used in this paper (Fig. 2) was mainly derived from the following references: Guérin (1980), Garutt (1994), Markovic (1998), Holbrook (2001), Antoine (2002), Qiu and Wang (2007), Tong and Guérin (2009), and van der Made (2010). Measurements of the teeth and bones were taken according to the methods of the following authors: Guérin (1980), Kahlke and Lacombat (2008), and van der Made (2010). All measurements are given in millimeters.

Abbreviations—**BMNH**, Beijing Museum of Natural History, Beijing, China; **BPI**, Bernard Price Institute for Paleontological

*Corresponding author.

Color versions of one or more of the figures in the article can be found online at www.tandfonline.com/ujvp.

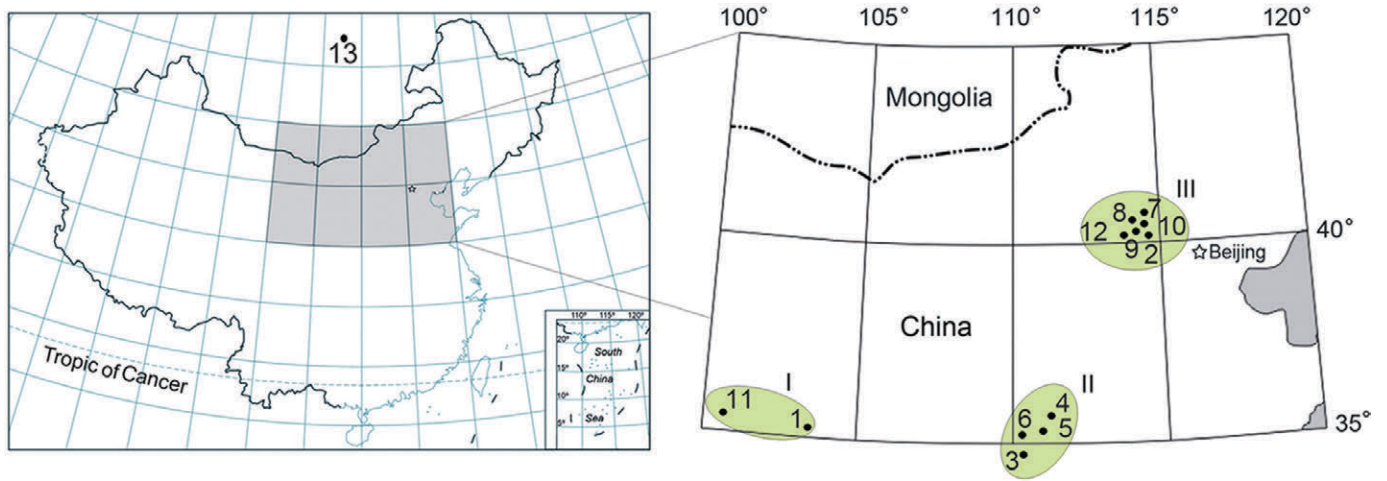


FIGURE 1. Map showing distribution of early Pleistocene *Coelodonta* in northeast Asia. **I**, Longdan; **2**, Danangou; **3**, Xihoudou (= Hsihoutu); **4**, Tunliu; **5**, Wenxi; **6**, Linyi; **7**, Xiashagou; **8**, Nihewan Village; **9**, Xiaochangliang; **10**, Shanshenmiaozui; **11**, Gonghe; **12**, Hutouliang; **13**, Western Transbaikalia. **I**, Qinghai; **II**, South Shanxi; **III**, Nihewan Basin.

Research, University of the Witwatersrand, Johannesburg, South Africa; **CKT**, Chou-kou-tien (=Zhoukoudian); **H**, height; **IVPP**, Institute of Vertebrate Paleontology and Paleoanthropology, Beijing, China; **Mc**, metacarpal; **Mt**, metatarsal; **MNHN**, Muséum National d'Histoire Naturelle, Paris, France; **MNQ**, Neogene and Quaternary Mammalian Biozones (Mammifères Néogènes et Quaternaires); **NHW**, Nihewan (= Nihowan); **SJA**, Sjarosso-gol, Inner Mongolia; **SSMZ**, Shanshenmiaozui; **TNP**, Tianjin Natural History Museum (= Musée Hoang ho Pai ho), Tianjin, China; **ZRC**, Zoological Reference Collection (National University of Singapore), Singapore.

SYSTEMATIC PALEONTOLOGY

Class MAMMALIA Linnaeus, 1758
 Order PERISSODACTYLA Owen, 1848
 Family RHINOCEROTIDAE Gray, 1821
 Subfamily RHINOCEROTINAE Gray, 1821
 Tribe DICERORHININI Loose, 1975
 Genus *COELODONTA* Bronn, 1831

Generic Diagnosis—See Qiu et al. (2004).
Included Species and Subspecies—*Coelodonta antiquitatis* (Blumenbach, 1799); *Coelodonta tologoiensis* Beliajeva, 1966;

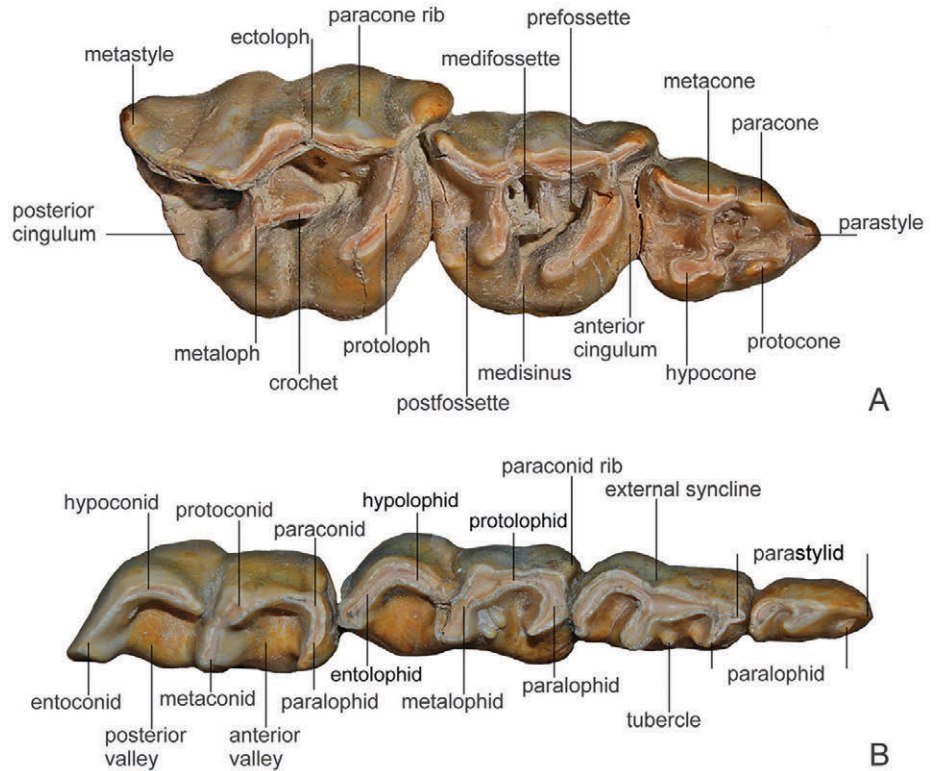


FIGURE 2. Dental nomenclature. **A**, upper cheek tooth; **B**, lower cheek tooth.

Coelodonta nihowanensis Kahlke, 1969; *Coelodonta antiquitatis shansius* Chia et Wang, 1978; *Coelodonta antiquitatis yenshanensis* Chow, 1979; *Coelodonta antiquitatis praecursor* Guérin, 1980; *Coelodonta thibetana* Deng et al., 2011.

COELODONTA NIHOWANENSIS Kahlke, 1969
(Figs. 2, 3, 4A, B, 5A–D, F, H, 7, 8, and 9B)

Rhinoceros cf. *tichorhinus* (Cuvier): Teilhard de Chardin and Piveteau, 1930:17–19, text-fig. 7, pl. II, figs. 3, 5, 7 and 9.
Coelodonta antiquitatis (Blumenbach, 1799): Li, 1984:64–65, pl. I, figs. 11–12.
Coelodonta antiquitatis (Blumenbach, 1799): Wei et al., 1985:227, pl. I, fig. 4.
Coelodonta antiquitatis (Blumenbach, 1799): Tang et al., 1995:79, pl. I, fig. 4.

Specific Diagnosis—See Qiu et al. (2004).

Referred Specimens—Juvenile cranium and mandible (IVPP V 17616.1, V 17616.2) with complete deciduous dentition (DP1–4/dp1–4); maxilla with DP1–3 (V 17616.3); partial cranium with DP1–4 (V 17616.4); broken mandible with dp3–4 (V 17616.5); partial right scapula (V 17616.6); cervical vertebrae C1–C6 (V 17616.7–12); deformed right humerus (V 17616.13); left radius (V 17616.14) and a distal radial epiphysis (V 17616.15); two broken ulnae (V 17616.16–17) and two left distal ulnar epiphyses (V 17616.18–19); two left pyramids (V 17616.20–21); left scaphoid (V 17616.22); two magnums (V 17616.23–24); left uncinate (V 17616.25); right semilunar (V 17616.26); left metacarpal II (V 17616.27), left Mc III (V 17616.28) and left Mc IV (V 17616.29); two tibiae (V 17616.30–31); right fibula (V 17616.32); right calcaneum (V 17616.33); four astragali (V 17616.34–37); right cuboid (V 17616.38); right Mt II (V 17616.39), right Mt III (V 17616.40), and right Mt IV (V 17616.41); phalanges 1–3 of foot digit III (V 17616.42–44).

Locality and Horizon—40°13'08"N, 114°39'54"E, Shanshenmiaozi, Yangyuan County, Hebei Province, China; early Pleistocene.

DESCRIPTION

Juvenile Cranium—The juvenile cranium is almost completely preserved, with slight damage to the zygomatic arch, the tip of the nasal, and the premaxilla. The nasal and frontal are slightly displaced from their natural positions. The deciduous dentition is quite well preserved (see Table S1 in Supplemental Data for measurements).

In dorsal view (Fig. 3A), the nasal bones widen in the caudal direction and the internasal and nasofrontal sutures remain unfused. The nasofrontal contact lies at the level of the anterior border of the lacrimal. There is no visible rugosity to mark the position of the nasal horn boss. The broadest part of the frontal corresponds with the level of the anterior border of the orbit. The sutures, including the interfrontal, nasofrontal, and frontoparietal, remain unfused. The frontoparietal suture is at the level of the narrowest part of the cranium and the anterior edge of the zygomatic process of the temporal. The dorsal surface of the frontal is flat. The frontal horn boss cannot be detected yet. The parietal has two halves and exhibits a butterfly-like outline in dorsal view. The sutures surrounding the parietal, including the sagittal, parietosquamosal, frontoparietal, and the parieto-interparietal ones, are not yet fused. The anterior boundary of the parietal is interrupted by a small indentation that accommodates the frontal process, whereas the posterior part of the bone forms a notch to receive the anterior part of the interparietal. The parietal ridges approach one another most closely at the level of the posterior concavity of the parietal. The interparietal is well developed and triangular in shape, forming a long interparietal process that fits into the posteromedian parietal notch.

In lateral view (Fig. 3B), the profile of the parietal is quite flat, whereas the anterior part of the frontal forms a slight convexity. The wing of the nasal contacts both the lacrimal and the maxilla. Because of breakage in the lacrimal area, however, the details of the nasal and maxillary contacts with the lacrimal are not very clear. The anterior part of the maxilla is broken. The sutures around the maxilla, including the nasomaxillary, lacrimomaxillary, and jugomaxillary ones, remain unfused. The maxilla and nasal form the floor and roof of the nasal notch, respectively. The nasal notch is high at the entrance, but declines toward the base. The zygomatic process of the maxilla arises from the level of DP4 and the anterior border of the orbit, whereas the posterior end of the nasal notch lies above DP3. The infraorbital foramen is relatively large. The lacrimal is horizontally elongated. The lacrimal or preorbital tubercle, below which is the lacrimal foramen, is well developed. The area of contact between the frontal and parietal is slightly concave. The postglenoid process is moderately developed. The external acoustic meatus is funnel-like, overhung by the temporal crest, and bordered inferiorly and posteriorly by the posttympanic process and anteriorly by the postglenoid process. The temporal crest meets the nuchal crest, whereas the posttympanic process contacts both the postglenoid process and the paroccipital one. The occipital crest extends upward and moderately backward. The temporal crest lies at a slightly higher level than the superior margin of the zygomatic arch, rather than much lower as in other genera. The posterior margin of the pterygoid plate is gently sloped backward. The posttympanic process is moderately developed, but the details of its contact with the paroccipital process are unclear because of breakage. It is certain, however, that the posttympanic process contacts the posterior margin of the postglenoid process and closes off the subaural channel.

In posterior or nuchal view (Fig. 4A1), the posterior part of the temporal and the posttympanic process as well as the occiput are visible. The outline of the occiput is trapezoidal. The nuchal crest at the superior margin of the occiput is convex rather than straight. The occiput is moderate in height. The occiput is composed of four parts: the supraoccipital, the two exoccipitals, and the basioccipital. Most of the sutures remain partly open. However, the suture between the interparietal and the supraoccipital is fused completely. The foramen magnum is large and pear-shaped. The occipital condyles and the paroccipital process are damaged.

In palatal view (Figs. 3C, 4B, 5A), the palatal surface is trench-like, with the middle part, including maxilla and horizontal part of the palatine, very flat and the alveolar process of the maxilla rising very sharply. The transverse palatine suture is straight, and the palatine foramen is small (Fig. 4B). The margin of palatine notch and the root of the zygomatic arch lie at the same level as DP4. The basioccipital is short, with a narrow keel on its anterior portion, and the basioccipital-basisphenoid contact lies at the same level as the postglenoid process. The choana is broad. The middle portion of the basisphenoid bears a keel, which is flanked by a narrow platform on either side. The vomer is damaged, and its form is not clear. A groove extends posteriorly from the opening of the large caudal alar foramen (alisphenoid canal). Because of damage, the position of the contact between the alisphenoid and the pterygoid is uncertain. The maximum width across the zygomatic arches occurs at the same level as the minimum width of the braincase.

In anterior view (Fig. 4A2), the nasal opening is broad, high, and nearly rounded, and the infraorbital foramen is large.

The Juvenile Mandible—A juvenile mandible discovered near the cranium exhibits approximately the same stage of tooth eruption, and definitely belongs to the same individual, although it was not preserved in articulation. Apart from slight damage to the tip of the mandibular symphysis and the coronoid process, the mandible is quite well preserved, and the left dp1–4, right

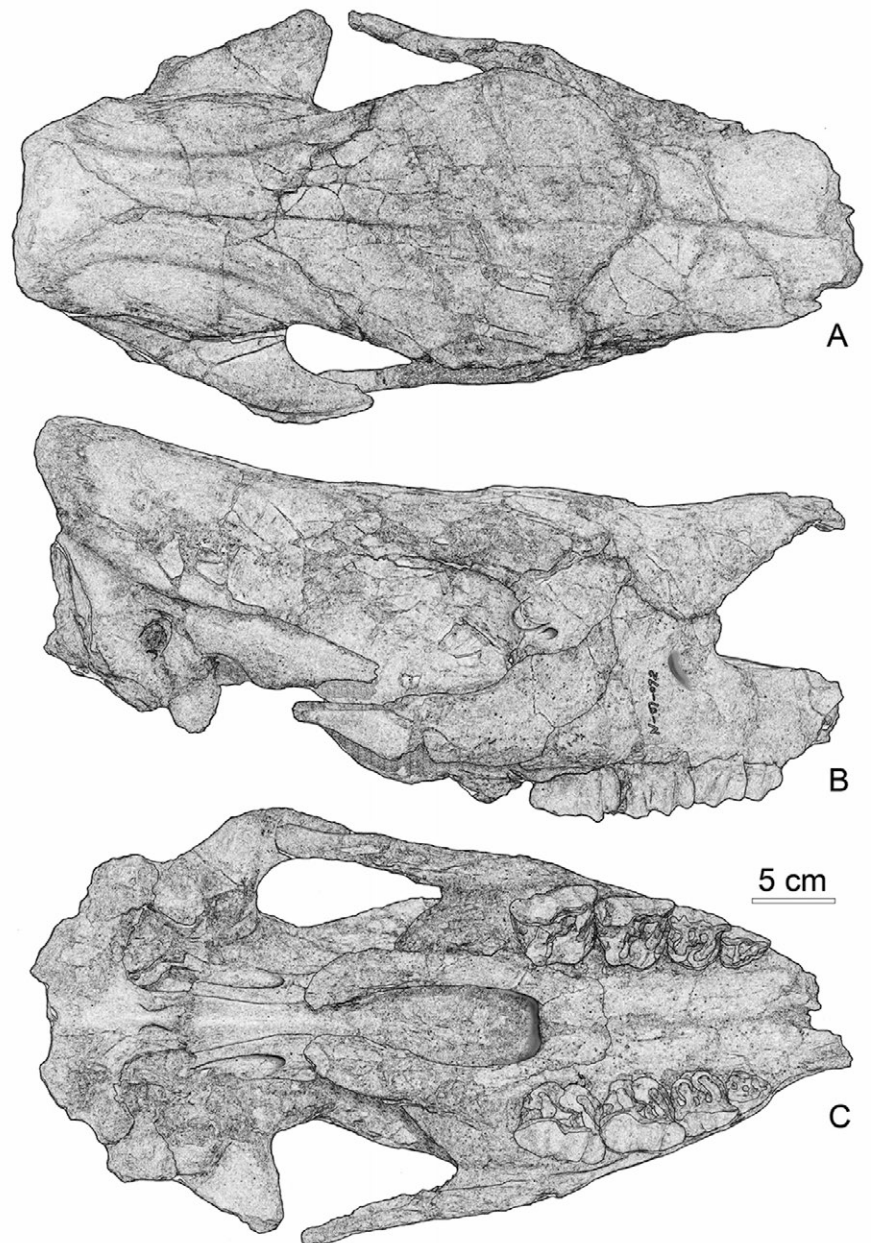


FIGURE 3. Juvenile cranium of *Coelodonta nihowanensis* from SSMZ, V 17616.1. **A**, dorsal view; **B**, lateral view; **C**, palatal view.

dp1, and right dp3–4 are all in situ. The mandibular symphysis is slightly constricted, and a vestigial di1 is visible in its alveolus (Fig. 5F3). The ventral surface bears some nutrient foramina. The inferior border of the slightly swollen mandibular body is nearly straight, but the anterior part is slightly elevated. The mental foramen is tiny and located just below dp1. On the lingual aspect, the mandibular foramen is located below the level of alveoli. The ascending ramus is inclined posteriorly. The dp1 is located posterior to the rear margin of the mandibular symphysis. The length and width of the mandibular symphysis are respectively 74 and 65, whereas the depth of the mandibular body at the level of dp4 is 64.7.

The dentition of the SSMZ skull shows features characteristic of tooth wear class IV as defined in *Ceratotherium simum*, which corresponds to an age of around 1.5 years according to Hillman-Smith et al. (1986). In accordance with the study of the dental

ontogeny of the woolly rhinoceros conducted by Garutt (1994), the SSMZ calves were 1.5–2.0 years old (stage C:I) when they died.

Upper Teeth—(See Figs. 2–5 and Table S2 in Supplemental Data for measurements.) Because the premaxilla was not preserved, the presence or absence of the upper deciduous incisors is not clear. Garutt (1994) reported that the upper milk incisors occurred in no more than 4% of the studied samples of *C. antiquitatis*.

The crown of DP1 has a triangular outline in occlusal view. The metacone and hypocone are very well developed; the paracone is less well developed, and located in a very posterior position; the protocone is tongue-like and in contact with both the parastyle and the hypocone, respectively, but also maybe isolated; the hypocone is in the form of a crest that is aligned perpendicular to the metaloph and extends forward to meet the

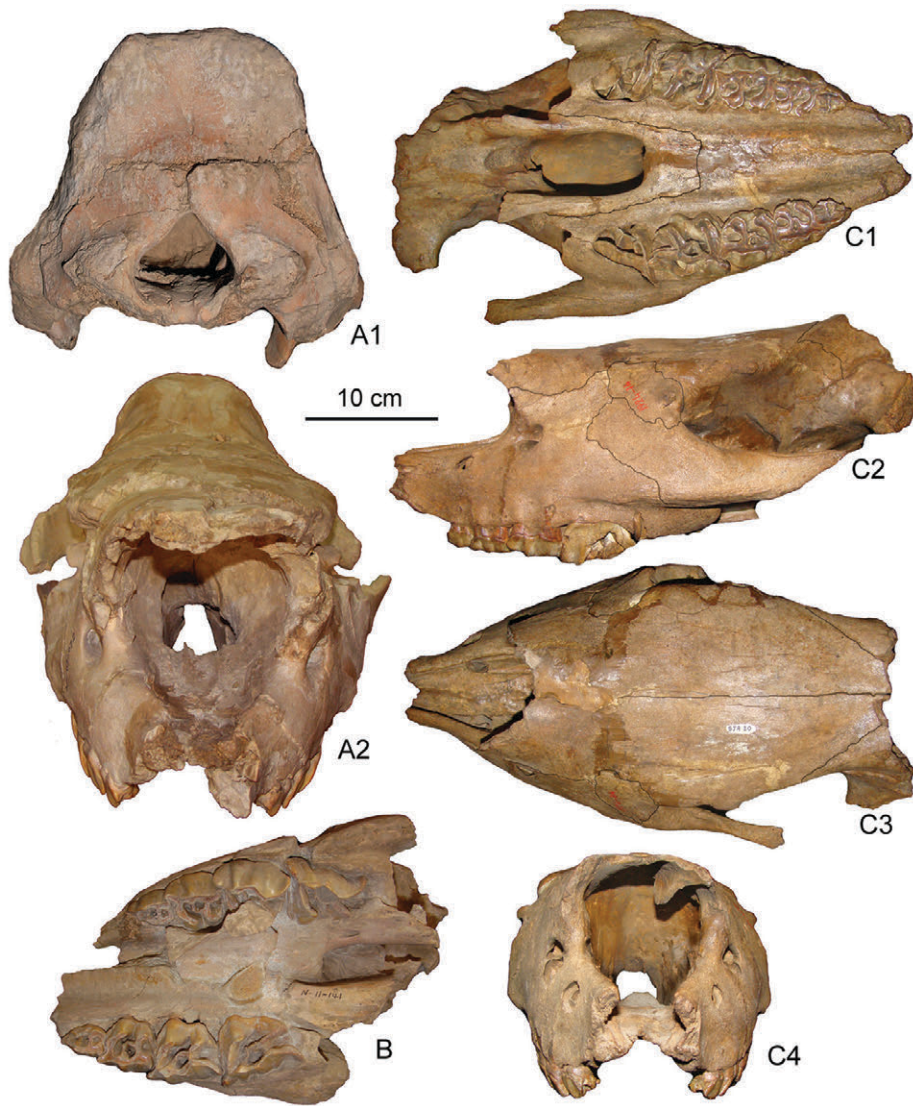


FIGURE 4. Juvenile crania of *Coelodonta nihowanensis* (A, B) and *Coelodonta antiquitatis* (C1-4). A, V 17616.1, from SSMZ; B, V 17616.4, from SSMZ; C, SJA 30, from Sjarosso-gol. A1, occipital view; A2 and C4, anterior views; B and C1, palatal views; C2, lateral view; C3, dorsal view.

protocone, closing off the medisinus. The parastyle is less well developed and in a much lower position than other main cusps before abrasion, a condition that represents one of the most important characters of *Coelodonta*. The ectoloph is developed. The protoloph (or paraloph) arises from the protocone, and contacts both the parastyle and the hypocone. The metaloph is poorly developed, resulting in the formation of an 'inner wall' through contact between the protoloph and the hypocone, and the angle between the 'inner wall' and the ectoloph is small. The crochet is quite close to the hypocone. In some cases, the crista and crochet are not in contact with each other, and the prefossette connects with the medifossette. In other cases, however, the crista contacts the protoloph, separating the trigon basin into a narrower prefossette and a broader medifossette. The lingual side of the protoloph bears a faint cingulum.

The crown of DP2 has a trapezoidal outline in occlusal view, with the buccal side longer than the lingual side and the maximum width occurring at the level of protoloph. The anterior margin is not straight. The main cusps are well developed, with the paracone located at the middle of the ectoloph. The profile of the ectoloph is wave-like, each cusp or style corresponding with a fold or rib on the ectoloph, and the paracone rib is the most

pronounced of these structures. The protoloph and metaloph are developed. The crochet and crista are also developed, and come together to form the medifossette. The medisinus is open. The anterior and posterior cingula are both developed, but the former is shorter. A weakly developed cingulum is present at the entrance of the medisinus.

The crown of DP3 also has a trapezoidal outline, with the buccal side longer than the lingual one. The main cusps are developed, with the paracone located in a relatively anterior position, but the styles are reduced. The situation of the profile of the ectoloph and the ribs are the same as in DP2. The protoloph is curved backward and is better developed than the metaloph. The crochet and crista are also developed, and come together to form the medifossette. The medisinus is open. Anterior and posterior cingula are developed, and the anterior cingulum bears a small tubercle.

DP4 is similar in morphology to DP3, but is a larger tooth. The main cusps are developed, with the paracone located more anteriorly than in DP3, but the styles are reduced. The ribs on the outer wall are not so pronounced as in DP3, and the protoloph is better developed than the metaloph. Anterior and posterior cingula are developed, and the latter bears an enamel tubercle.

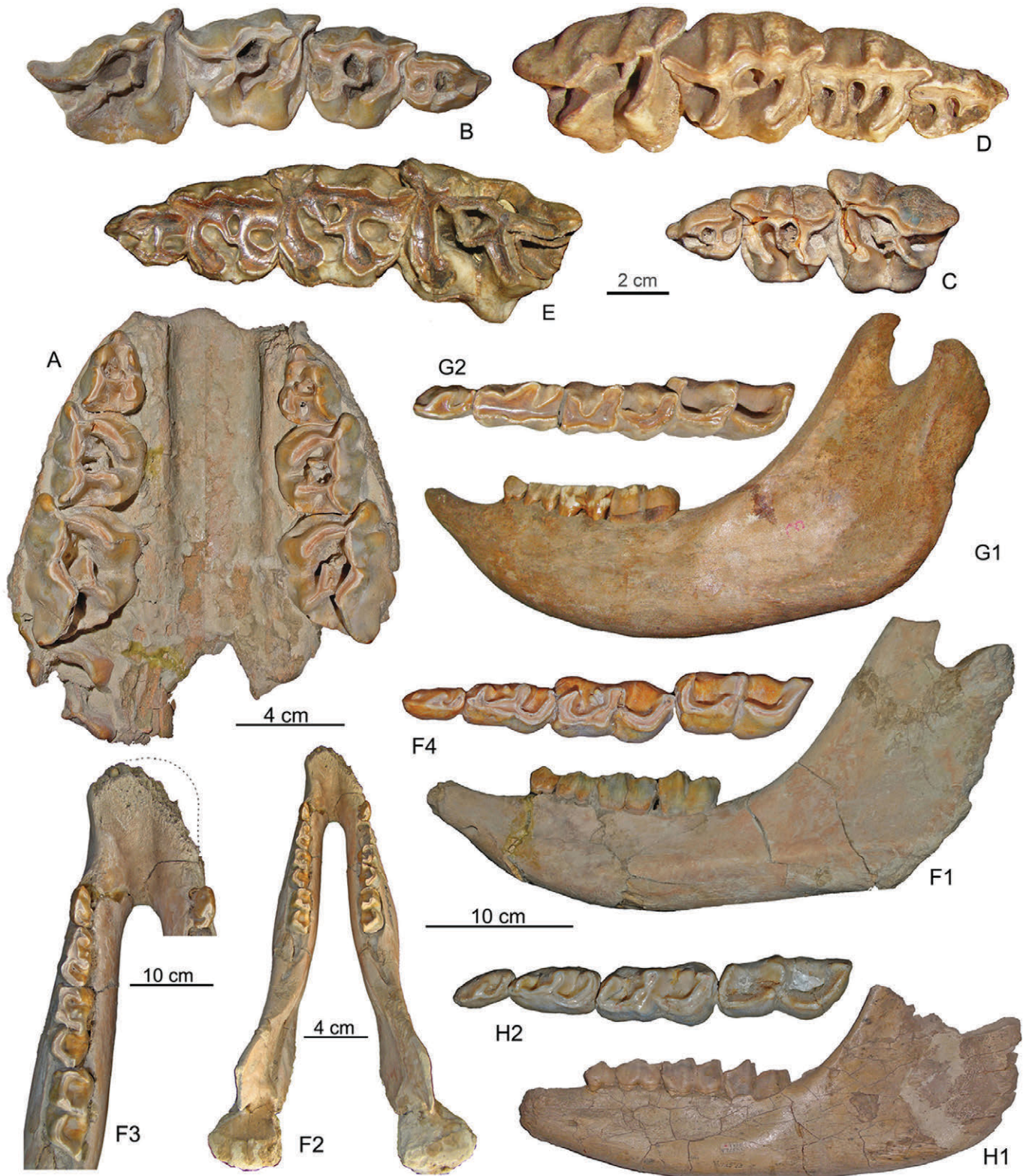


FIGURE 5. Juvenile maxilla, mandible, and deciduous teeth of *Coelodonta nihowanensis* (A–D, F, and H), compared with those of *Coelodonta antiquitatis* (E and G). A, maxilla with DP1–3 (V 17616.3); B, details of right DP1–4 (V 17616.4); C, left DP1–3 (V 7257-1); D, details of right DP1–4 (TNP 00196); E, details of left DP1–4 (SJA 30); F, mandible with dp1–4 and di1 (V 17616.2); G, mandible with dp1–4 (Inner Mongolia Museum, no catalog number); H, left mandible with dp1–4 (V 7257-3). A, B, F, from SSMZ; C, H, from Danangou; D, from Xiashagou; E, G, from Sjara-osso-gol in Ordos. A–E, F2–4, G2, H2, crown views; F1, G1, H1, buccal views. Images F4, H2, G2 are twice enlarged relative to the scale bar.

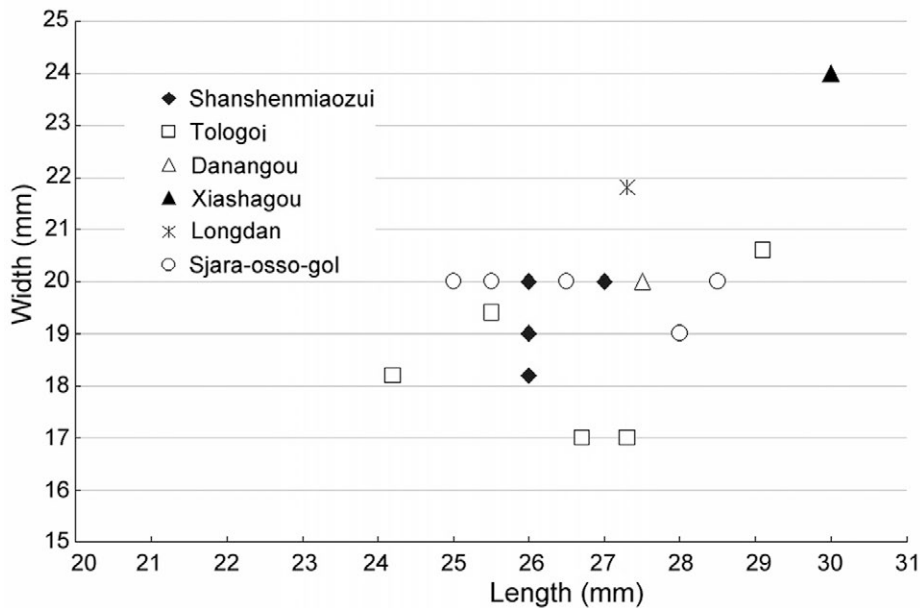


FIGURE 6. Bivariate scatter plot of measurements of DP1 in different species of *Coelodonta*. Measurements of the Tologoi DP1 were taken from the figures of Belayeva (1966).

The characters of the upper deciduous teeth can be summarized as follows: the enamel surface is rough with little cement, the outer wall of the ectoloph is rugose, and the length/width ratio of the crown is large. The total length of DP1–4 is 136.

Lower Teeth—(See Figs. 2 and 5 and Table S3 in Supplemental Data for measurements.) The di1 is peg-like, with a sharp tip and a diameter of 5.

The dp1 is simply constructed, and tongue-like in form. The anterior valley is not ‘U’-shaped. The cuspids other than the paraconid are developed. Although the paralophid is only incipient and the protolophid is poorly developed, the other lophids are well developed. The surface of the ectolophid (protolophid + hypolophid) is flat, and the external syncline is not pronounced. The posterior valley is narrow, with its entrance located quite far posteriorly, and intersects the longitudinal axis of the crown at a small angle.

The dp2 is twice as large as dp1, and has two complete lobes. The major cuspids are quite well developed, and a cristid erupting from the paraconid is termed the parastyloid in this paper. The lophids are also developed, with the exception of the paralophid, which may be absent (MNHN NIH 086) or weak (MNHN NIH 084; V 17616.2). The surface of the ectolophid is not flat. The anterior valley is open, with enamel tubercles at the entrance, and the posterior valley is narrow but quite deep.

The dp3 is obviously larger than dp2 and is also more molarized, with a better-developed paralophid. However, the parastyloid of dp3 has disappeared, and the paraconid rib is more prominent than that of dp2. Both valleys of dp3 are broad, and the enamel tubercles at the entrance are much bigger than in dp2.

The dp4 is the same size as dp3, or slightly larger, and is completely molarized, but less hypsodont than the permanent molars; the cuspids and lophids are quite well developed. Both valleys of dp4 are broad, but lack enamel tubercles at their entrances.

Collectively, the lower teeth are characterized by the following features: rough and uneven tooth surfaces, a high degree of molarization, not flared tooth crown, and strong development of the paraconid. Among the lower deciduous teeth, a parastyloid is present only in dp2 and dp3, but in the former tooth this structure is very well developed. All of the lower deciduous teeth (dp1–4) are double-rooted. The combined length of dp1–4 is 130.

Postcrania—(Figs. 7, 8; see Table S4 in Supplemental Data for measurements.) The atlas (Fig. 7A, B) is distinct in appearance from the other cervical vertebrae in having neither centrum nor transverse foramen. In the specimen V 17616.7, the transverse process is damaged, but the articular surface and dorsal and ventral arches are well preserved. In dorsal view, an alar notch between the cranial surface and the transverse process is visible; the cranial notch is shallow, but the caudal notch is deep and irregular in form. The dorsal tubercle is robust, with a rough surface. A suboccipital foramen (Prothero, 2005), also known as the alar foramen (Guérin, 1983), is present on each side of the dorsal tubercle at the same level as the alar notch, opening to the side and connecting to the vertebral canal. In ventral view, a developed, posteriorly protruding ventral tubercle is visible. In anterior view, two kidney-shaped facets for articulation with the occipital condyles can be observed on the cranial surface, lateral to the vertebral foramina and separated from each other by superior and inferior notches. The caudal surface of the atlas articulates with the axis and is irregular in form, but much flatter; the two lateral facets are connected by the facet for the dens; the lower portion of the vertebral canal becomes narrower, where the dens is housed. The measurements are as follows: height 125, length >110, width >196, and widths of anterior and posterior articular surfaces 150 and 134, respectively. All of these measurements fall within the known ranges of the corresponding ones for *C. antiq-uitatis* from Western Europe (Guérin, 1983).

The structures of the axis (Fig. 7A, C) include the dorsal arch, centrum, vertebral canal, transverse foramen, neural spine, odontoid process, and posterior articular process. No anterior articular process is present, and both the transverse process and the transverse foramen are small. The vertebral body tapers anteriorly to form the protruding odontoid peg. The centrum is opisthocoeleous, and has a keel-like ventral surface. The measurements of the axis are as follows: total length 131, width of the anterior articular facet 59, and width of the posterior articular facet 129.

Other cervical vertebrae, including C3 to C6 (Fig. 7A), are also preserved. In dorsal view, the anterior and posterior articular processes have a butterfly-like shape in outline. The neural spines are very damaged. The articular facet of the anterior articular process faces upward and has the shape of an irregular

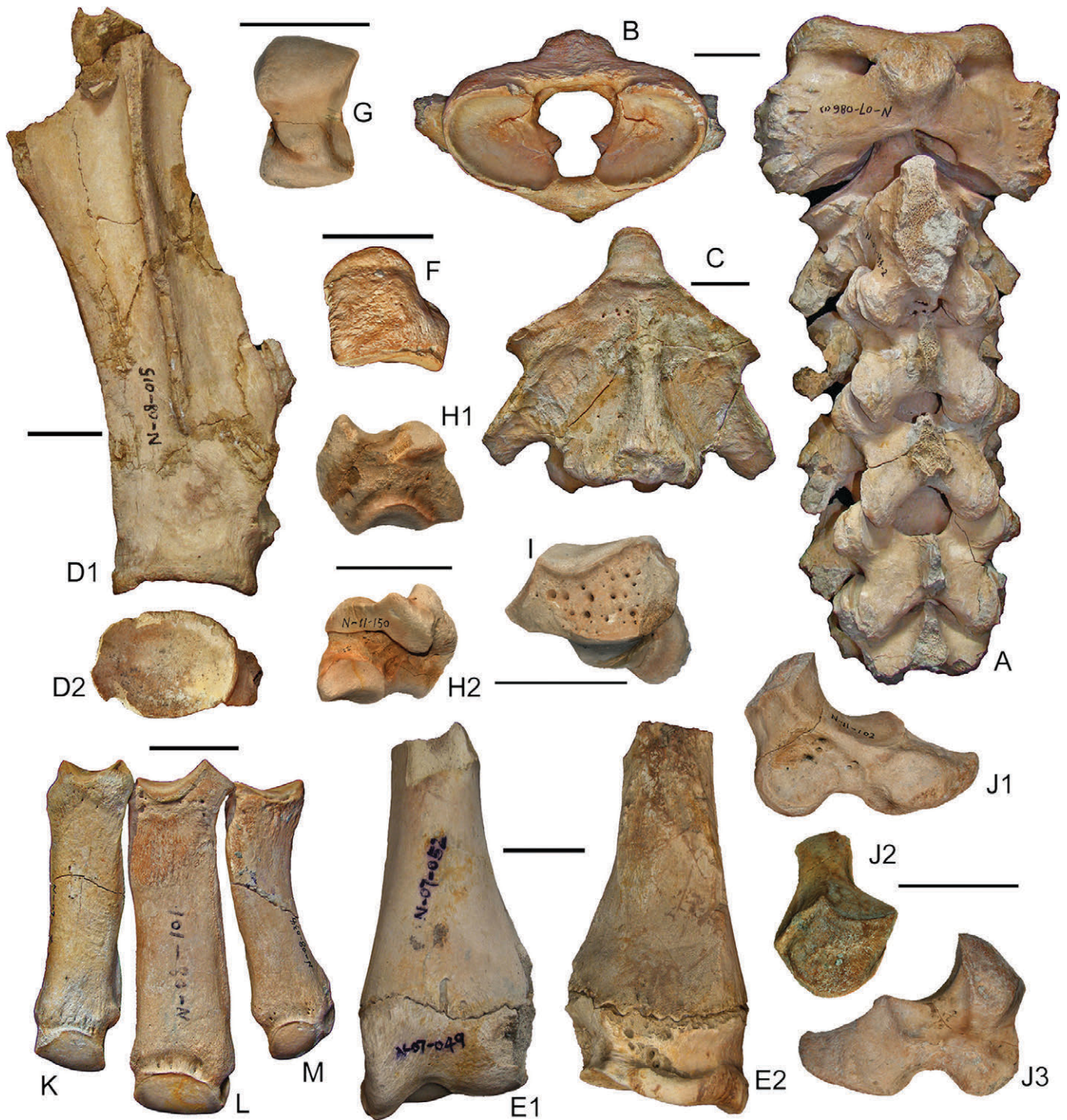


FIGURE 7. Vertebrae and forelimb bones of *Coelodonta nihowanensis* from SSMZ. **A**, cervical vertebrae I–VI (V 17616.7–12), dorsal views; **B**, atlas (V 17616.7), cranial view; **C**, axis (V 17616.8), ventral view; **D1–2**, right scapula (V 17616.6), lateral and distal views; **E1–2**, left radius (V 17616.14), anterior and posterior views; **F**, left pyramidal (V 17616.20), dorsal view; **G**, left semilunar (V 17616.26), posterior view; **H**, left scaphoid (V 17616.22), dorsal and lateral views; **I**, left uncinates (V 17616.25), dorsal view; **J1–3**, right magnum (V 17616.23), medial, dorsal, and lateral views; **K**, left Mc II (V 17616.27); **L**, left Mc III (V 17616.28); **M**, left Mc IV (V 17616.29). **K–M**, dorsal views. Scale bars equal 50 mm.

polygon, but that of the posterior articular process faces downward and is nearly round. The transverse foramen increases in size from C3 to C5, but becomes smaller again in C6. The centrum of each postaxial cervical is anteriorly convex and posteriorly concave, with a keeled ventral surface. However, the keel is less pronounced in the more posterior vertebrae.

The blade of the only available scapula (Fig. 7D) has been damaged over most of its surface, but parts of the spine and the glenoid area are still intact. The preserved part of the caudal border of the blade is nearly straight. Both the coracoid process and the supraglenoid tubercle are invisible. The articular surface has a transverse diameter of 69 and an anteroposterior diameter of 94.

The single humerus specimen is strongly compressed except at its distal end. Both the coronoid and olecranon fossae are very deep. No supratrochlear foramen is present. In anterior view, the trochlea is very similar to that of the astragalus, and is divided by a saddled groove into a stronger medial condyle and a smaller, ridge-like lateral one. The medial condyle has a height of 101, and the lateral condyle height is 73. Both the medial epicondyle and the lateral one are damaged. The humerus (MNHN NIH 154) from Xiashagou has strongly inclined trochlear ridges. The total length of the SSMZ humerus exceeds 433 (the length of the Xiashagou humerus, for comparison, is 440), and the transverse diameter of the distal articular surface is 99.

The radius (Fig. 7E) is represented only by the distal epiphysis and part of the shaft. These portions of the radius are detached from each other, implying that the bone is from a juvenile or a subadult. In form, the radius resembles those of the later woolly rhinos. The distal transverse diameter is 104, slightly larger than in the SJA specimen, but within the range seen in specimens from Xiashagou (82–115) (Teilhard de Chardin and Piveteau, 1930). The distal articular surface has a length of 95 and a width of 56, dimensions that slightly exceed those of the specimens from SJA. However, they fall within the ranges seen in the woolly rhinos from Western Europe, in which the length and width of the distal articular surface respectively measure 76.5–116 and 44–63.5 (Guérin, 1980).

A partial ulna lacking the distal end and olecranon is present in the sample. This bone resembles its counterpart in the late *Coelodonta* from Sjara-osso-gol in both morphology and size, apart from having a less well developed lateral coronoid process.

The pyramidal or cuneiform (Fig. 7F) is very similar in morphology to its counterpart in other rhinos, apart from having larger articular facets on the medial surface. The proximal articular facet (ulnar facet) becomes narrow but uplifted at the rear part. The distal articular surface has the approximate outline of a rounded triangle.

The semilunar or lunar bone (Fig. 7G) has a crescentic (half-moon) shape in lateral or medial view. The proximal surface bears a broad and irregular convex facet for the radius. The medial surface contacts the scaphoid, and the lateral surface contacts the pyramidal. The superior edge of the dorsal surface is much larger than the inferior one. The distal surface is composed of two concave facets: the mediolateral facet articulates with the magnum, and the laterodistal facet articulates with the unciform. In lateral view, a long volar process can be observed.

One juvenile or subadult scaphoid (Fig. 7H) is available. The proximal face of the scaphoid is entirely occupied by the facet for the radius. This facet is essentially concave, with a median anteroposteriorly trending valley, but the lateral half of the facet for the radius is convex. On the lateral face are two narrow facets for contact with the lunar bone. There are two distal facets, one for the magnum and one for the trapezoid.

The unciform or uncinete (Fig. 7I) is very similar in morphology to specimens of the same bone in *C. antiquitatis*, having broad proximal and medial articular surfaces. The dorsal surface has many foramina. The volar process is robust.

The adult magnum (Fig. 7J) has a fairly long posterior tubercle (or volar process). This bone bears a proximal facet for the scaphoid, a lateral facet for the unciform, and a distal facet for Mc III. A juvenile magnum is remarkably smaller, and has a much shorter volar process.

Mc II (Fig. 7K) was recognized during preparation in the laboratory. This bone is slightly smaller than Mc III and quite straight, with a proximal articular surface (for articulation with the trapezoid) that is small and ear-shaped. The facets for contact with the magnum and Mc III are connected, forming a continuous surface. Bulges occur on the medial and posterior sides of the proximal end.

Mc III (Fig. 7L) is broad, flat, and straight, and the proximal end of this bone bears five facets. The medial facet contacts Mc II, the proximal facet is the largest and contacts the magnum, the two lateral facets contact Mc IV, and the proximolateral facet contacts the uncinete.

Mc IV (Fig. 7M) is markedly smaller than Mc III, with a bent shaft and a pronounced notch on the lateral side. The proximal end bears three facets; the proximal facet is the largest and contacts the uncinete. The two proximomedial facets contact Mc III.

The tibia (Fig. 8A) is preserved intact. In anterior view, it is evident that the cnemial crest or tibial tuberosity is moderately developed at the proximal end, and that the groove for middle patellar ligament does not extend far downward. At the distal end of the tibia, the medial malleolus is not developed. In posterior view, the popliteal fossa is moderately pronounced, but the popliteal line is not prominent. A tongue-shaped process arises from the medioposterior edge of the distal end and extends downward, fitting into the median groove of the astragalus. In lateral view, the proximal articular facet for the fibula is not well defined, but the distal facet is pronounced. The proximal articular surface of the tibia is broad, and is divided into medial and lateral condyles by an intercondylar eminence. The tibial tuberosity is continuous with the lateral condyle, forming a nearly straight proximolateral margin. The popliteal notch is not deep, whereas the intercondylar eminences are moderately high and pronounced. The intercondylar sulcus is pronounced, but not deep, and extends to the popliteal notch. The distal articular surface has the outline of an irregular quadrilateral, with the lateral edge being the shortest. The articular fossa is not very deep. A crista intermedia lies near the medial side of the articular surface and divides it into two portions, of which the medial one is narrower transversely, longer anteroposteriorly, and much deeper. The tibia is longer and more slender than those of European *Coelodonta* specimens.

The proximal end of the fibula (Fig. 8B) is absent, and the length of the preserved shaft and distal end is 250. The distal end measures 50 anteroposteriorly and 21 transversely. The distal articular surface for the tibia measures 37×22 , values close to those of *C. antiquitatis* given by Borsuk-Bialynicka (1973).

Only one calcaneum (Fig. 8E) was recovered. The calcaneal tuberosity, a moderately long process, has a slightly expanded end and is obviously less mediolaterally compressed than in *C. antiquitatis* specimens from Sjara-osso-gol. The calcaneum bears three surfaces that articulate with the astragalus: the lateral astragalus, sustentacular, and distal astragalus facets. The lateral astragalus facet consists of two parts that meet at an obtuse angle and correspond to the lateral calcaneal facet of the astragalus. The sustentacular facet is almost flat. The distal astragalus facet is a narrow strip and confluent with the cuboid facet. The distal articular surface, a kidney-shaped facet for the cuboid, is concave anteroposteriorly and the entire facet rises posteriorly.

The astragalus (Fig. 8D) is preserved intact. As in other rhinos, the astragalus is of the single-pulley type; the trochlea is not symmetrical, with the lateral ridge being broader than the medial one. The medial and lateral ridges are parallel to each other, but slightly oblique to the long axis of the bone. In the specimens from Xiashagou (e.g., MNHN NIH 070), the lateral ridge is obviously higher than the medial one, but in the specimens from SSMZ the lateral ridge is slightly higher than the medial one. The neck of the astragalus is higher medially than laterally, and the medial side bears a tuberosity. In plantar view, three articular surfaces can be observed: the proximal calcaneal, sustentacular, and distal calcaneal facets. The proximal calcaneal facet is large and concave. The sustentacular facet is a flat oval, whereas the distal calcaneal facet looks like a drop and is confluent with the distal part of the sustentacular facet. In distal view, two facets can be distinguished: a medial one for the navicular and a lateral one (combined with the distal end of calcaneum) for the cuboid; the

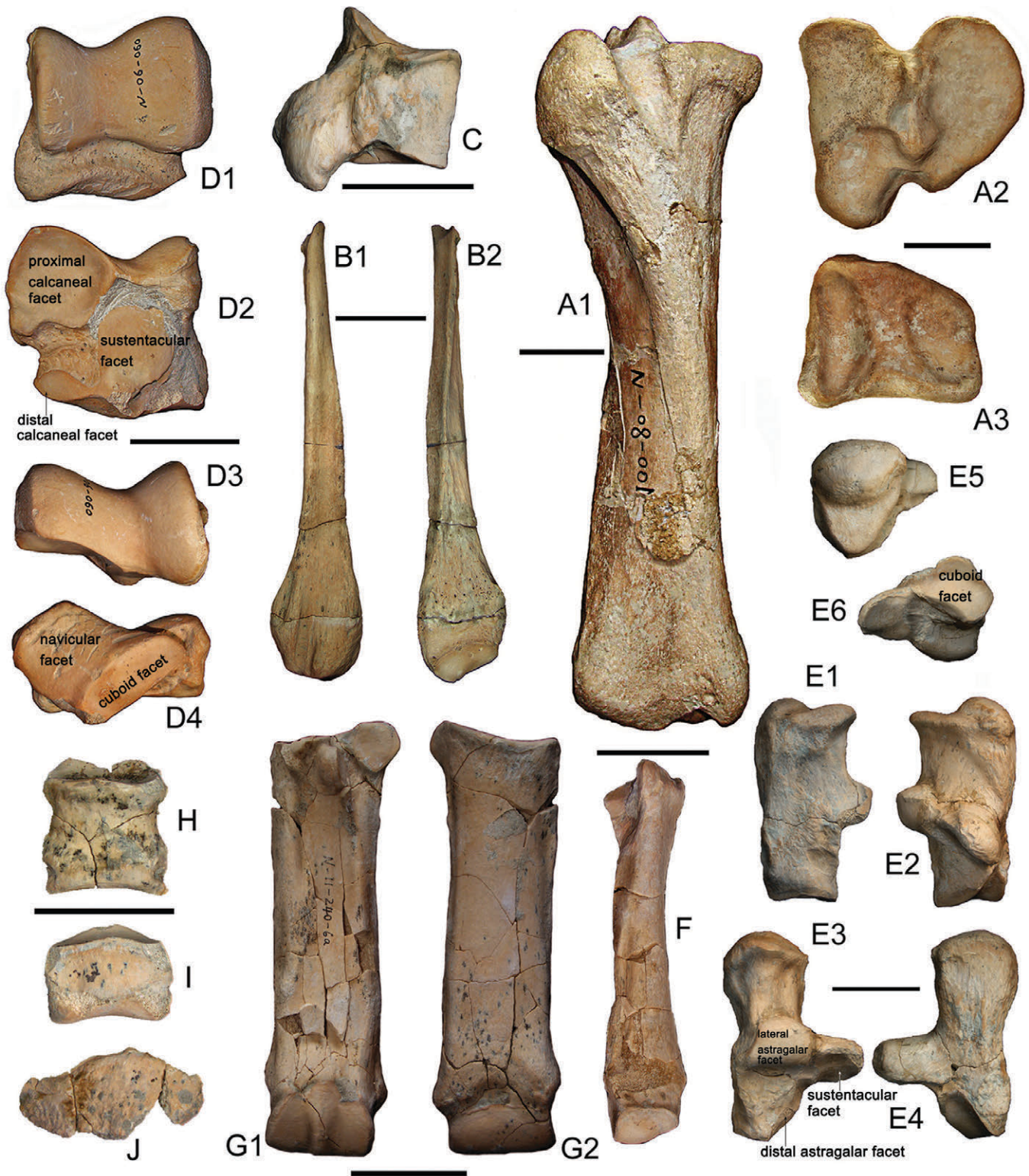


FIGURE 8. Hind limb bones of *Coelodonta nihowanensis* from SSMZ. **A1–3**, right tibia (V 17616.30); **B1–2**, right fibula (V 17616.32); **C**, right cuboid (V 17616.38); **D1–4**, left astragalus (V 17616.34); **E1–6**, right calcaneum (V 17616.33); **F**, right Mt II (V 17616.39); **G1, 2**, right Mt III (V 17616.40); **H–J**, 1st (V 17616.42), 2nd (V 17616.43), and 3rd (V 17616.44) phalanges of digit III. **A1**, anterior view; **A2, D3, E5**, proximal views; **A3, D4, E6**, distal views; **B1, C, E1**, lateral views; **B2, E2**, medial views; **D1, E3, F, G2, H–J**, dorsal views; **D2, E4, G1**, plantar views. Scale bars equal 50 mm.

two facets consist of a large, irregular four-sided polygonal continuous surface, the anterior edge of which is the longest, and is nearly straight.

The proximal facet of the cuboid is concave, for articulation with both the calcaneum and the astragalus. Two medial facets for articulation with the ectocuneiform and navicular are present, as is a distal facet for articulation with the fourth metatarsal. The plantar or volar process is robust (Fig. 8C).

The proximal facet of Mt II is kidney-shaped and articulates with the mesocuneiform. It bears two small lateral facets that articulate with the ectocuneiform. The distal end bears a large rounded trochlea (Fig. 8F) for articulation with the first phalanx; the keel on the plantar surface lies to the medial side.

Mt III has a very anteroposteriorly compressed shaft. The proximal facet is very broad and flat, and articulates with the ectocuneiform. Two small, subcircular lateral facets articulate with Mt IV. The anterior surface of the distal trochlea is flat, but the plantar surface bears a medial keel (Fig. 8G).

Proximal, medial, and distal phalanges (Fig. 8H–J) of the same individual are represented among the material from SSMZ, but show no specialized features.

COMPARISONS AND DISCUSSION

Identification of the Rhino Fossils from Shanshenmiaozui

The rhino fossils from SSMZ can be referred to *C. nihowanensis* based on the following features: lacrimal large and longitudinally elongated, upper deciduous teeth have large length/width ratio, developed parastyle, DP1 triangular in outline with reduced protocone, DP2 with pronounced paracone rib, dp1 and dp2 complex in structure, lower incisors rudimentary, paralophid developed, with rugose enamel and rough outer wall of crown, mandibular body slightly thickened, and ascending ramus of mandible slopes backward. Although some of the characters mentioned above also correspond with equivalent ones of *C. antiquitatis*, some other qualitative characters, e.g., a lower degree of hypsodonty, developed cingula, less backward curved protoloph on the upper teeth, and slender limb bones, support a tentative assignment of the SSMZ specimens to *C. nihowanensis* Kahlke, 1969.

The following comparisons are in chronological order of the taxa and the morphological relationships; the less related and more primitive taxa will appear first.

Comparisons with *Stephanorhinus*

Among all rhinocerotid taxa, *Elasmotherium* and *Coelodonta* have the most specialized teeth. But *Stephanorhinus* is commonly regarded as the genus most closely related to *Coelodonta* (Groves, 1983; Cerdeño, 1995; Deng et al., 2011); and some authors have proposed that “*Stephanorhinus* shares important characteristics with *Coelodonta*” (van der Made, 2010:446). Therefore, it is worth making some comparisons between the two genera.

With regard to cranial features, *Stephanorhinus* has a proportionally higher and shorter skull than *Coelodonta*. The occipital crest is less posteriorly inclined, the postglenoid process is more robust, the temporal crest is shorter and positioned lower than the superior margin of zygomatic process of temporal bone (Fig. 9C), the infraorbital foramen is located in a more anterior position and is almost invisible in lateral view, and the lacrimal bone is triangular (Fig. 10C). By contrast, in *Coelodonta*, the temporal crest is nearly at the same level or higher than the superior edge of the zygomatic process of squamosal (Fig. 9A, B), with the longitudinal axis of the lacrimal bone more horizontally directed (Fig. 10A, B). In *Stephanorhinus*, only the anterior portion of the nasal septum is ossified, whereas ossification of the septum is normally complete in adult specimens of *Coelodonta*,

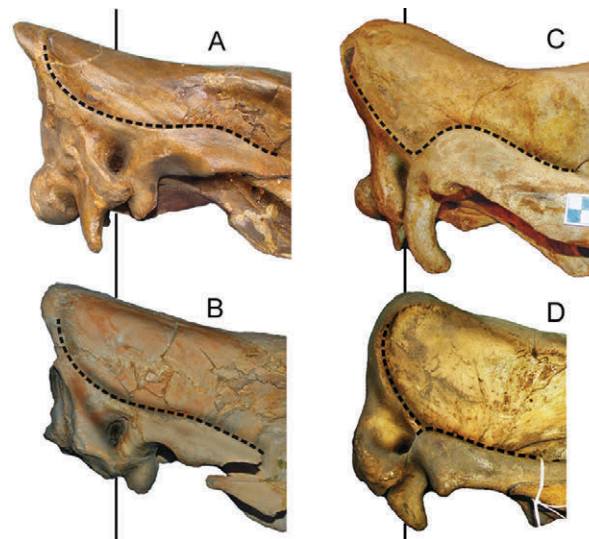


FIGURE 9. Comparisons of the morphology of the supra-aural region and the location of the external auditory meatus among some juvenile rhinoceroses (not to scale); it seems that only in *Coelodonta* the temporal crest is positioned higher than zygomatic process of temporal bone. **A**, *Coelodonta antiquitatis* from late Pleistocene Dingcun site, V 1453; **B**, *Coelodonta nihowanensis* from SSMZ, V 17616.1; **C**, *Stephanorhinus kirchbergensis* from Shennongjia, SNHM H36; **D**, *Rhinoceros sondaicus*, extant, MNHN A7966.

and the foramen magnum is approximately round (Tong and Wu, 2010), rather than pear-shaped as in *Coelodonta* (Fig. 4A1). The mandible of *Stephanorhinus* lacks incisors entirely and has a more constricted symphysis than is present in *Coelodonta*, whereas the latter genus retains rudimentary incisors in some cases and has a more posteriorly inclined ascending ramus.

Among the deciduous teeth, DP1 of *Stephanorhinus* has stronger transverse crests, which are parallel with each other; a relatively posteriorly positioned metaloph and hypocone; a less developed crochet and crista; and a posteriorly opened post-fossette. By contrast, *Coelodonta* has less developed transverse crests, and the protoloph meets the metaloph at the lingual side of the crown. In DP2, the paracone rib is located in the middle of the ectoloph, rather than in the anterior one-third as in *Stephanorhinus*. Furthermore, a parastylid is only present on dp2 in *Coelodonta*, rather than on both dp2 and dp3 as in *Stephanorhinus*, and in *Coelodonta* the only lower teeth without paraconid ribs are dp1 and p2.

Comparisons with *Coelodonta* Fossils of Early to Middle Pleistocene Age

Occurrences of early *Coelodonta* in China mainly occur in three regions: the Nihewan Basin (sensu lato), southern Shanxi (Tunliu, Wenxi, Linyi, and Xihoudu), and the Qingzang Plateau (Longdan, Gonghe and others) (Fig. 1). *Coelodonta* may also occur in the Yushe Basin (Teilhard de Chardin, 1936), but this discovery has never been reported in detail. The only area outside China to have yielded early *Coelodonta* is the Transbaikal Region, where the stratigraphically lowest occurrence of *Coelodonta* can be correlated with the *Coelodonta*-producing beds at Nihewan. Comparisons between the SSMZ specimens and those from other early *Coelodonta* localities are drawn below. Unfortunately, existing descriptions of the deciduous teeth of *Coelodonta* are very insufficient (Garutt, 1994), which limits the amount of detail in the following comparisons.

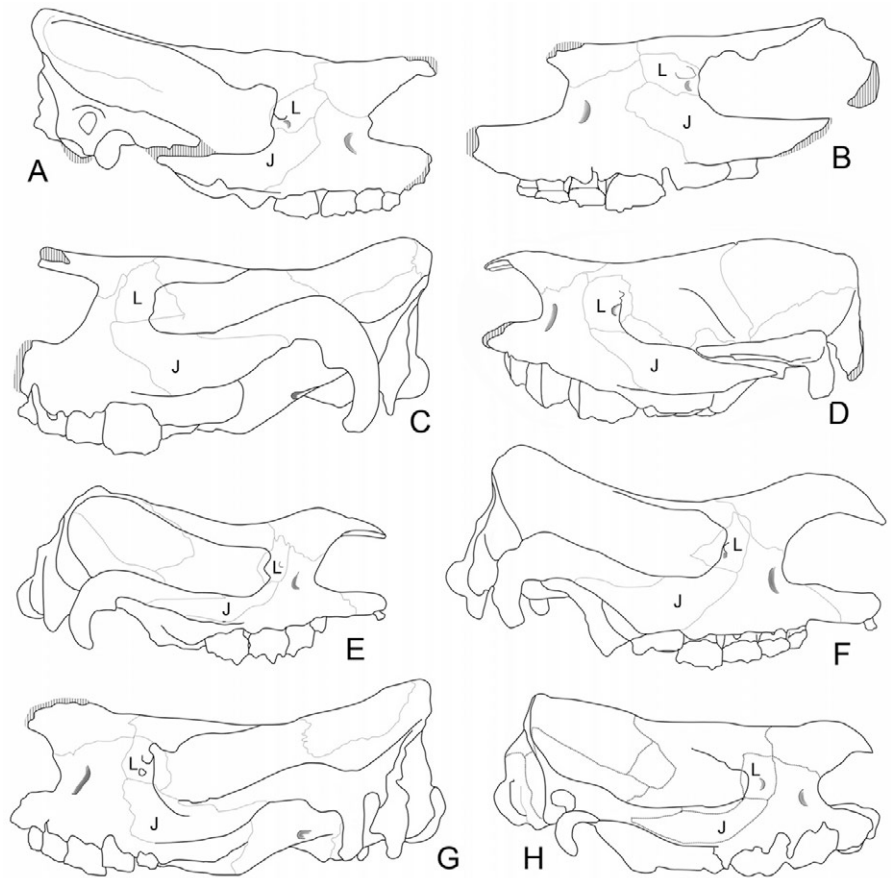


FIGURE 10. Comparisons of lacrimal-jugal contact patterns among juvenile rhinos (not to scale). **A**, *Coelodonta nihowanensis*, based on specimen V 17616.1 from SSMZ; **B**, *Coelodonta antiquitatis*, based on specimen SJA 30 from the Upper Pleistocene; **C**, *Stephanorhinus kirchbergensis*, with P4 fully erupted, based on specimen SNHM H36 from Shennongjia, Upper Pleistocene; **D**, *Dicerorhinus sumatrensis*, DP4 not fully erupted, based on specimen ZRC.4.1977 from Singapore, extant; **E**, *Rhinoceros sondaicus*, juvenile, extant; **F**, *Rhinoceros unicornis*, based on specimen IVPP OV 1046, extant; **G**, *Ceratotherium simum*, based on specimen from BPI, no catalog number, extant; **H**, *Diceros bicornis*, juvenile, extant. **E** and **H** are modified from Blainville (1841). In **A**, **B**, **D**, **E**, **F**, **G**, and **H**, the only functional teeth are deciduous. Fine lines represent the sutures, and the hatched areas indicate damaged regions. **Abbreviations**: **L**, lacrimal; **J**, jugal.

Comparisons with *Coelodonta thibetana* from Tibet—*Coelodonta thibetana* Deng et al., 2011, the most primitive *Coelodonta* species, comes from the Pliocene of Tibet and was described only recently (Deng et al., 2011). This species is represented only by an adult specimen, making comparisons with the SSMZ specimens difficult, but some comments are necessary. Based on its general morphology, *C. thibetana* can be securely retained in the genus *Coelodonta*. However, this species lacks some characteristic features of other species in this genus, in that the nasal septum is not completely ossified, the outline of M3 in occlusal view is triangular, and the cheek teeth have poorly developed buccal ribs.

Comparisons with ‘*Coelodonta nihowanensis*’ from Longdan—The ‘*C. nihowanensis*’ material from Longdan differs from the SSMZ specimens in that the ascending ramus is less posteriorly inclined, the mandibular symphysis is less constricted, the deciduous tooth row is longer, and the length/width ratio of each tooth crown is smaller. In addition, the enamel is less wrinkled, the cement is thinner, and the ribs on the buccal surface of the cheek teeth are less well developed. The DP1 lacks crochets, is buccolingually wide, and has better-developed lingual cusps, a crown whose outline is not a typical triangle, developed cingula, and a less well developed crista. The protoloph of DP2 is not strongly kinked as in *C. antiquitatis*.

Comparisons with *Coelodonta antiquitatis shansius* Chia and Wang, 1978—Because of the lack of known deciduous teeth and postcranial fossils of *C. antiquitatis shansius* from Xihoudu, southern Shanxi, it is not easy to compare this species with the SSMZ specimens. Specifically, *C. antiquitatis shansius* is a large taxon with the following distinctive characteristics: nasal bone

long and obviously extending anteriorly beyond the premaxilla but not bending at the tip, resulting in the formation of large nasal apertures; the occipital crest with strong posterior inclination, resulting in an angle of less than 40° between the parietal plane and the occipital surface; and metaloph remains on M3, probably because of the developed “metacone rib” (Cerdeño, 1995:10) or the “newly formed metastyle” (Heissig, 1989:413). The presence of these specialized features led Chia and Wang (1978) to erect the new subspecies *C. antiquitatis shansius*. The geologic age of the Xihoudu (Hsihoutu) Fauna is still disputed. It can be biostratigraphically correlated with CKT Locality 12, whose age is 2.0–1.8 Ma (Chia and Wang, 1978; Qiu, 2006). Additional *Coelodonta* localities such as Linyi and Wenxi have been discovered in the vicinity of the Xihoudu site, but the fossils from these sites are limited to isolated teeth and jaw fragments.

Comparisons with Fossils from Other Nihewan Basin Localities—In China, the known early *Coelodonta* localities are quite concentrated in the Nihewan Basin, including Danangou (Li, 1984), Xiashagou (Teilhard de Chardin and Piveteau, 1930), Xiaochangliang (Tang et al., 1981, 1995), Donggutuo (Wei et al., 1985), and Hutouliang (Pei, 2001). The early *Coelodonta* fossils from Nihewan once were grouped together with those from Gonghe in the distinct species *C. nihowanensis* (Kahlke, 1969; Chow, 1979), which has also been considered to include recently recovered primitive *Coelodonta* specimens from Longdan (Deng, 2002; Qiu et al., 2004). However, this species name is still open to question according to the rules of nomenclature, because neither type locality nor type specimen was ever designated, nor was any description or diagnosis provided, although a lectotype from Longdan was designated later and the emended diagnostic

characters were mainly based on the specimens from Longdan (Qiu et al., 2004). Accordingly, it has been proposed that *C. nihowanensis* should be treated as a nomen nudum (Kahlke, 2004). Additionally, some of the specimens that have been assigned to *C. nihowanensis* are very similar to *C. antiquitatis*, and have even been included in the latter species without discussion by some authors (Li, 1984). This may be the result of the ongoing disputes surrounding the taxonomy of the early woolly rhinos from the Nihewan Basin.

Among the *Coelodonta* localities in Nihewan, only Xiashagou and Danangou have yielded juvenile fossils. These specimens are very similar to those from SSMZ, apart from their slightly larger deciduous dentition, but all of them fall within the range seen in *C. antiquitatis* and have developed buccal ribs on their teeth. The fossils from Hutouliang, a locality of relatively young age (end of the early Pleistocene), are nearly identical to the late Pleistocene *Coelodonta* specimen. Additionally, the postcranial elements (humeri, radii, ulnae, metacarpals, femora, tibiae, metatarsals, etc.), known from Xiashagou are very similar to those from SSMZ, and all of them also fall within the range of variation characteristics of *C. antiquitatis* (Guérin, 1980) with respect to both qualitative characters and proportions. On average, postcranial bones from Xiashagou are larger than those of late Pleistocene European woolly rhinos, rather than smaller as previously believed.

In conclusion, all the early Pleistocene *Coelodonta* specimens from Nihewan Basin can be included in the species *C. nihowanensis*, but the type material should be selected from the type locality.

Comparisons with *Coelodonta tologojensis* from Transbaikalia—*Coelodonta tologojensis* was established by Belayeva (1966) based on specimens from the early middle Pleistocene fossil layer Tologoi 2.5, located on the bank of the Selenga River in western Transbaikalia. Subsequent discoveries show that the temporal range of *Coelodonta* in this region may extend back to 1.8 Ma BP, which corresponds to MN18 (Alexeeva and Erbajeva, 2000). The diagnostic characters of this species only include “not so massive as *C. antiquitatis*, and with slender limb bones” (Belayeva, 1966:98) as the species was established. The Tologoi DP1 specimens have relatively smaller size than the specimens from other regions (Fig. 6). In addition, *C. tologojensis* has a better-developed protocone and a more posteriorly located contact point with the ectoloph, resulting in the formation of an anterior gulf, and no structure extends anteriorly from the hypocone. Another pronounced difference between *C. tologojensis* and *C. nihowanensis* is the less well developed paracone rib in the former. Unfortunately, the cranial material from the type locality of *C. tologojensis* is insufficient for detailed comparisons, rendering the morphology and phylogenetic position of this species somewhat unclear.

Comparisons with *Coelodonta antiquitatis* from Gonghe—The Gonghe Basin in Qinghai Province yields the best preserved and richest early to middle Pleistocene *Coelodonta* fossils, which include four crania and a broken mandible, but there are few deciduous teeth available for comparison with those of SSMZ specimens. According to the descriptions and images published by Zheng et al. (1985), the two complete adult crania from Gonghe can be placed uncontroversially within the species *C. antiquitatis*. These specimens are not as large as those from Sjava-osso-gol, but still fall within the size range of the late *C. antiquitatis* from Europe. However, it once was proposed that the *Coelodonta* fossils from Gonghe should be included in the species *C. nihowanensis*, mainly because of their lower stratigraphical position and smaller size (Chow, 1978).

Comparisons with *Coelodonta antiquitatis yenshanensis* Chow, 1978—Chow (1979) established the subspecies *C. antiquitatis yenshanensis* based on specimens from CKT Localities 1,

9, and 13 of middle Pleistocene, and summarized the diagnosis of the subspecies as follows: skull, teeth, and limb bones smaller than that of *C. antiquitatis*; M3 triangular, with relatively brachydont teeth, a thinner enamel layer, and an outer wall with enamel pillars or tubercles. It is noteworthy that the only cranium (Chow, 1979:pl. 1, figs. 1, 2; VM.555; housed in the Geological Museum of China) recovered at CKT Locality 1 was referred to *Dicerorhinus choukoutienensis*. However, we believe that it is probably referable to *C. antiquitatis* because the angle between the parietal plane and occipital surface is small, the occipital crest has a strong posterior inclination, the junction between the temporal crest and the zygomatic process of squamosal is very smooth, the infraorbital foramen is located more posteriorly than in *Stephanorhinus*, and the occipital crest is wide and straight.

Comparison with *Coelodonta antiquitatis praecursor* Guérin, 1973—In 1973, Guérin reported the rhino fauna from La Fage, the late middle Pleistocene (ca 0.25 Ma) site that has yielded the richest assemblage of *C. antiquitatis* material known from Europe up to that time. He subsequently named the subspecies *Coelodonta antiquitatis praecursor* based on specimens from this site (Guérin, 1980). This subspecies can be distinguished from the typical woolly rhino by its more slender limb bones, and comes from the biozone MNQ24. Because insufficient deciduous teeth are known for *Coelodonta antiquitatis praecursor*, the only common character shared by the new subspecies and *C. nihowanensis* is the slenderness of the limb bones.

Comparison with Late Pleistocene *Coelodonta antiquitatis* (Blumenbach, 1799)—Although Late Pleistocene *C. antiquitatis* specimens have been divided into various types or subspecies (Borsuk-Bialynicka, 1973; Jiang, 1977), they are united by some unique characters. The SSMZ specimens share many characters with *C. antiquitatis*: flat skull roof profile in lateral view, temporal crest nearly at same level as superior edge of zygomatic arch, occipital crest and nuchal surface slope backward, foramen magnum pear-shaped, ascending ramus slopes backward, incisors vestigial or lost, with wrinkled dental enamel, buccal walls of cheek teeth bear strong folds or ribs, crochets and cristae developed, and protolophids straight (Figs. 2, 5).

The early Pleistocene forms display some subtle differences from later examples of *C. antiquitatis*: cement on tooth surfaces thin or absent, crista of DP1 usually meets crochet, rather than protoloph as in late woolly rhinos, anterior cingulum better developed, posterior valley on dp1 not closed, less hypsodont; slightly more slender limb bones.

Discussion

Groves (1983) and Prothero et al. (1986) considered *Coelodonta* to be the sister taxon of *Stephanorhinus*. Cerdeño (1995) also identified *Stephanorhinus* as the closest relative of *Coelodonta*, but she combined these taxa with the sister-group pair of *Ningxiatherium* and *Elasmotherium* to form the subtribe Elasmotheriina. Prothero et al. (1986) also considered *Elasmotherium* to be very close to the sister taxa *Coelodonta* and *Stephanorhinus*. *Coelodonta* shares such characteristics with some species of the genus *Stephanorhinus* as with both nasal and frontal horns, horn bosses are rugose, without front teeth; occipital plane inclined moderately to strongly backward. On the other hand, *Coelodonta* resembles *Elasmotherium* in having a completely ossified nasal septum and hypsodont cheek teeth with cement and corrugated enamel surfaces. Finally, *Coelodonta* resembles the extant rhino *Ceratotherium* in having a subquadrate M3, dolichocephalic skull, hypsodont teeth, and posteriorly inclined occipital surface.

The phylogenetic position of the genus *Coelodonta* is less controversial than the interrelationships of the various species within this genus. *C. tibetana* should be the chronologically earliest species, and the crucial characters seen in this taxon are

entirely primitive apart from the strong backward inclination of the nuchal crest. The *C. nihowanensis* specimens from Longdan represent another primitive form within the genus *Coelodonta*, but also resemble *Stephanorhinus* in having a less backwardly inclined nuchal crest and in many other features. Strictly speaking, these specimens can be regarded as an intermediate type positioned between *Stephanorhinus* and typical *Coelodonta* in morphology. It is difficult to group the fossils from Longdan with those from Nihewan and Gonghe that have been assigned to *C. nihowanensis* and *C. antiquitatis*, respectively. A reasonable solution to this problem might be to establish a new species for the fossils from Longdan, but such a revision lies beyond the scope of the present paper.

Some authors have proposed that the earliest westward dispersal into Europe of *C. tologojensis*, the early *Coelodonta* species known from the Transbaikalian region, took place in the early middle Pleistocene (about 0.46 Ma BP) and led to the subsequent origin of the true woolly rhino in Europe. The earliest record of *Coelodonta* in Europe is from the Bad Frankenhausen locality in Germany (Kahlke and Lacombat, 2008). Results of the present study agree that *C. antiquitatis* originated much earlier in China, as previously proposed (Teilhard de Chardin and Piveteau, 1930; Prothero et al., 1989). However, currently available data are still insufficient to comprehensively reconstruct the evolutionary history of *Coelodonta*, particularly given that the species *C. nihowanensis* and *C. tologojensis* are not well represented in the fossil record. Actually, except the species *C. antiquitatis*, other species referred to the genus *Coelodonta* are not well defined because of insufficient fossil material.

CONCLUSIONS

The qualitative characters and proportions of the *Coelodonta* fossils from the lower Pleistocene deposits in Nihewan Basin support tentative referral of these materials to the species *C. nihowanensis*. These specimens also fall within the range of variation seen in *C. antiquitatis* with regard to most of their features, but differ from the latter species in the following respects: less hypsodont cheek teeth, better-developed cingula, protoloph less strongly curved back, and more slender limb bones.

Among the SSMZ rhino fossils, the most significant individual specimens are the juvenile crania and mandibles, as well as the deciduous teeth. The juvenile skull described in this paper represents the most complete and youngest (around 1.5 years old) cranial specimen of an early woolly rhino ever discovered.

The present authors believe that the presence of an extremely backward inclined occipital plane can be employed as a crucial diagnostic character of the genus *Coelodonta*. The general characteristics of this genus also include the completely ossified nasal septum in adult, dolichocephalic skull, temporal crest positioned higher than zygomatic process of temporal bone, subquadrate M3 (i.e., with developed metastyle), hypsodont cheek teeth with cement and corrugated enamel surfaces, lower cheek teeth with prominent paraconid ribs, and longitudinal axis of the lacrimal bone extending more horizontally. The primitive species *C. thibetana* from Tibet and *C. nihowanensis* from Longdan still lack some of the crucial characters of the true woolly rhino, such as their nasal septa are not completely ossified, M3 teeth are still triangular in occlusal outline, and cheek teeth with poorly developed buccal ribs. Some authors have proposed that the woolly rhino originated in northern China, and then dispersed into northern Eurasia. In this scenario, *C. nihowanensis* gave rise to *C. tologojensis*, which in turn gave rise to *C. antiquitatis* (Deng, 2008; Kahlke and Lacombat, 2008). However, the phylogenetic position of *C. tologojensis* is still open to question because of the insufficient representation in the fossil record. Among the known early Pleistocene *Coelodonta* fossils in China, those

from the Nihewan Basin most closely resemble the true woolly rhinos.

ACKNOWLEDGMENTS

The authors would like to thank the following persons and institutions: F. Han, Z.-J. Xu, N. Hu, X. Chen, and C. Yin for field work; Prof. Q. Wei for providing information on the SSMZ site; V. V. Titov for providing access to literature; C. Argot of MNH, M. Zheng of TPN, and Z.-H. Zeng of BMNH for hosting the first author during collections visits; H. Li from the Inner Mongolia Museum for providing some specimens for comparison; and T.-T. Lim for providing images of the juvenile Sumatran rhino. The authors are also very grateful to Z.-X. Qiu for reading the first draft of the manuscript and making constructive suggestions; to X.-M. Wang, T. Deng, and R.-D. Kahlke for constructive suggestions and fruitful discussions; to the JVP editors B. Van Valkenburgh and J. Harris as well as X.-M. Wang and an anonymous reviewer for their constructive suggestions, and to Dr. C. Sullivan for improving the English text. This work was supported by the Key Research Program of the Chinese Academy of Sciences (grant no. KZZD-EW-15), the Project from the P.R.C. Ministry of Land and Resources (grant no. 201211005-3), and the IVPP Project (grant no. KN213413), as well as the special fund for fossil excavation and preparation of the Chinese Academy of Sciences.

LITERATURE CITED

- Antoine, P. O. 2002. Phylogénie et évolution des Elasmotheriinae (Mammalia, Rhinocerotidae). Mémoires du Muséum Nationale d'Histoire Naturelle de Paris 188:1–359.
- Belayeva (= Beliajeva), E. I. 1966. Rhinocerotidae; pp. 92–133 in E. A. Vangengeim, E. I. Beliajeva, and V. E. Garutt (eds.), Eopleistocene Mammals of Western Transbaikalia. NAUKA, Moscow. [Russian]
- Blainville, H. M. D. de. 1841. Ostéographie, ou description iconographique, mammifères. Arthus Bertrand, Paris, Rhinoceros PL II–III.
- Borsuk-Bialynicka, M. 1973. Studies on the Pleistocene rhinoceros *Coelodonta antiquitatis* (Blumenbach). Palaeontologia Polonica 29:1–94.
- Boule, M., H. Breuil, E. Licent, and P. Teilhard de Chardin. 1928. Le Paléolithique de la Chine. Archives de Institut de Paléontologie Humaine, Mémoire 4:1–136.
- Bronn, H. G. 1831. Über die fossilen Zähne eines neuen Geschlechtes aus der Dickhaute-Ordnung *Coelodonta* Hohlenzahn. Jahrbuch für Mineralogie, Geognosie, Geologie und Petrefaktenkunde 2:51–61.
- Cerdeño, E. 1995. Cladistic analysis of the family Rhinocerotidae (Perissodactyla). American Museum Novitates 3142:1–25.
- Chia, L.-P., and C. Wang. 1978. Hsihoutu—A Culture Site of Early Pleistocene in Shansi Province. Cultural Relics Publishing House, Beijing, 85 pp. [Chinese 1–82; English 83–85]
- Chow, B.-S. 1978. The distribution of the woolly rhinoceros and woolly mammoth. Vertebrata Palasiatica 16:47–59. [Chinese 47–58; English 59]
- Chow, B.-S. 1979. The fossil rhinocerotids of locality 1, Choukoutien. Vertebrata Palasiatica 17:236–258. [Chinese 236–255; English 256–258]
- Deng, T. 2002. The earliest known woolly rhino discovered in the Linxia Basin, Gansu Province, China. Geological Bulletin of China 21:604–608. [Chinese 604–607; English 608]
- Deng, T. 2008. Comparison between woolly rhino forelimbs from Longdan, Northwestern China and Tologoi, Transbaikalian region. Quaternary International 179:196–207.
- Deng, T., X.-M. Wang, M. Fortelius, Q. Li, Y. Wang, Z. J. Tseng, G. T. Takeuchi, J. E. Saylor, L. K. Säilä, and G.-P. Xie. 2011. Out of Tibet: Pliocene woolly rhino suggests high-plateau origin of ice age megaherbivores. Science 333:1285–1288.
- Erbajeva, M. A., and N. V. Alexeeva. 2000. Pliocene and Pleistocene biostratigraphic succession of Transbaikalia with emphasis on small mammals. Quaternary International 68:67–75.
- Garutt, N. V. 1994. Dental ontogeny of the woolly rhinoceros *Coelodonta antiquitatis* (Blumenbach, 1799). Cranium 11(1):37–48.

- Gray, J. E. 1821. On the natural arrangement of vertebrate animals. London Medical Repository 15, April 1:297–310.
- Groves, C. P. 1983. Phylogeny of the living species of rhinoceros. *Zeitschrift für Zoologische Systematik und Evolutionforschung* 21:293–313.
- Guérin, C. 1973. Les trois espèces de rhinoceros (Mammalia, Perissodactyla) du gisement pléistocène moyen des Abimes de La Fage (Corrèze). *Nouvelles Archives du Muséum d'Histoire naturelle de Lyon*, Fasc. 11:55–84.
- Guérin, C. 1980. Les rhinocéros (Mammalia, Perissodactyla) du Miocène Terminal au Pléistocène Supérieur en Europe Occidentale: comparaison avec les espèces actuelles. *Documents des Laboratoires de Géologie de Lyon* 79(1–3):1–1185.
- Guérin, C. 1983. Le gisement Pléistocène Supérieur de la Grotte de Jaurès à Nespoules, Corrèze, France: les Rhinocerotidae (Mammalia, Perissodactyla). *Nouvelles Archives du Muséum d'Histoire Naturelle de Lyon* 21:65–85.
- Heissig, K. 1989. The Rhinocerotidae; pp. 399–417 in D. R. Prothero and R. M. Schoch (eds.), *The Evolution of Perissodactyls*. Oxford University Press, New York.
- Hillman-Smith, A. K. K., N. Owen-Smith, J. L. Anderson, A. J. Hall-Martin, and J. P. Selaladi. 1986. Age estimation of the white rhinoceros (*Ceratotherium simum*). *Journal of Zoology* 210:355–377.
- Holbrook, L. T., 2001. Comparative osteology of early Tertiary tapiriforms (Mammalia, Perissodactyla). *Zoological Journal of the Linnean Society* 132:1–54.
- Jiang, P. 1977. A new subspecies of *Coelodonta antiquitatis*. *Vertebrata Palasiatica* 15:207–210. [Chinese]
- Kahlke, H.-D. 1969. Die Rhinocerotiden-Reste aus den Kiesen von Süßenborn bei Weimar. *Paläontologische Abhandlungen A* 3:667–709.
- Kahlke, R.-D. 2004. Bibliography 1951–2004 of Hans-Dietrich Kahlke; pp. 31–54 in L. C. Maul and R.-D. Kahlke (eds.), 18th International Senckenberg Conference, Weimar, 25–30 April 2004. *Terra Nostra*, Schriften der Alfred-Wegener-Stiftung 2004/2.
- Kahlke, R.-D., and F. Lacombat. 2008. The earliest immigration of woolly rhinoceros (*Coelodonta tolojensis*, Rhinocerotidae, Mammalia) into Europe and its adaptive evolution in Palaeartic cold stage mammal faunas. *Quaternary Science Review* 27:1951–1961.
- Li, Y. 1984. The Early Pleistocene mammalian fossils of Danangou, Yuxian, Hebei. *Vertebrata Palasiatica* 22:60–68. [Chinese 60–67; English 68]
- Linnaeus, C. 1758. *Systema Naturae* (10th edition). Holmiae, Laurentii Salvii, 824 pp.
- Loose, H. 1975. Pleistocene Rhinocerotidae of W. Europe with reference to the recent two-horned species of Africa and S.E. Asia. *Scripta Geologica* 33:1–59.
- Markovic, A. 1998. Woolly rhinoceros *Coelodonta antiquitatis* (Blumenbach, 1803) from Pleistocene of Serbia. *Bulletin of the Natural History Museum of Belgrade (A)* 47–50:217–237.
- Owen, R. 1848. Description of teeth and portions of jaws of two extinct Anthracotherioid quadrupeds (*Hyopotamus vectianus* and *Hyop. bovinus*) discovered by the Marchioness of Hastings in the Eocene deposits on the NW coast of the Isle of Wight: with an attempt to develop Cuvier's idea of the Classification of Pachyderms by the number of their toes. *Quarterly Journal of the Geological Society of London* 4:103–141.
- Pei, S.-W. 2001. Discovery of *Coelodonta antiquitatis* from Hutouliang in Nihewan Basin. *Vertebrata Palasiatica* 39:72–75. [Chinese 72–74; English 74–75]
- Pei, W.-C. 1958. Description of mammalian fossils; pp. 21–74 in W. C. Pei (ed.), *Report on the Excavation of Palaeolithic Sites at Tingsun, Hsiangfensien, Shansi Province, China*. *Memoirs of Institute of Vertebrate Paleontology and Paleoanthropology, Academia Sinica* (2). Science Press, Beijing. [Chinese 1–66; English 67–74]
- Prothero, D. R. 2005. *The Evolution of North American Rhinoceroses*. Cambridge University Press, Cambridge, U.K., 218 pp.
- Prothero, D. R., C. Guérin, and E. Manning. 1989. The history of the Rhinocerotidae; pp. 322–340 in D. R. Prothero and R. M. Schoch (eds.), *The Evolution of Perissodactyls*, Clarendon Press, New York.
- Prothero, D. R., E. Manning, and C. B. Hanson. 1986. The phylogeny of the Rhinocerotidae (Mammalia, Perissodactyla). *Zoological Journal of the Linnean Society* 87:341–366.
- Qiu, Z.-X. 2006. Quaternary environmental changes and evolution of large mammals in North China. *Vertebrata Palasiatica* 44:109–132.
- Qiu, Z.-X., and B.-Y. Wang. 2007. Paraceratheres fossils of China. *Palaeontologia Sinica New Series C* No. 29:1–396. [Chinese 1–248; English 249–396]
- Qiu, Z.-X., T. Deng, and B.-Y. Wang. 2004. Early Pleistocene mammalian fauna from Longdan, Dongxiang, Gansu, China. *Palaeontologia Sinica New Series C* No. 27:1–198. [Chinese 1–156; English 157–198]
- Tang, Y.-J., Y. Li, and W.-Y. Chen. 1995. Mammalian fossils and the age of Xiaochangliang Paleolithic Site of Yangyuan, Hebei. *Vertebrata Palasiatica* 33:74–83. [Chinese 74–82; English 83]
- Tang, Y.-J., Y.-Z. You, and Y. Li. 1981. Some new fossil localities of Early Pleistocene from Yangyuan and Yuxian Basin, Northern Hopei. *Vertebrata Palasiatica* 19:256–268. [Chinese 256–267; English 268]
- Tang, Y.-J., G.-F. Zong, and Q.-Q. Xu. 1983. Mammalian fossils and stratigraphy of Linyi, Shanxi. *Vertebrata Palasiatica* 21:77–86. [Chinese 77–85; English 85–86]
- Teilhard de Chardin, P. 1936. Fossil mammals from locality 9 of Choukoutien. *Palaeontologia Sinica Series C* 7(4):1–61.
- Teilhard de Chardin, P., and J. Piveteau. 1930. Les mammifères fossiles de Nihewan (Chine). *Annales de Paléontologie* 19:1–134.
- Tong, H.-W., and C. Guérin. 2009. Early Pleistocene *Dicerorhinus sumatrensis* remains from the Liucheng *Gigantopithecus* Cave, Guangxi, China. *Geobios* 42:525–539.
- Tong, H.-W., and X.-Z. Wu. 2010. *Stephanorhinus kirchbergensis* (Rhinocerotidae, Mammalia) from the Rhino Cave in Shennongjia, Hubei. *Chinese Science Bulletin* 55:1157–1168.
- Tong, H.-W., N. Hu, and F. Han. 2011. A preliminary report on the excavations at the Early Pleistocene fossil site of Shanshenmiaozui in Nihewan Basin, Hebei, China. *Quaternary Sciences* 31:643–653. [Chinese 643–652; English 653]
- van der Made, J. 2010. The rhinos from the Middle Pleistocene of Neumark-Nord (Saxony-Anhalt); pp. 433–527 in Mania, D. et al. (eds), *Neumark-Nord: Ein interglaziales Ökosystem des mittelpaläolithischen Menschen*. Veröffentlichungen des Landesmuseums für Vorgeschichte 62.
- Wei, Q., H. Meng, and S.-Q. Cheng. 1985. New Palaeolithic site from the Nihewan (Nihewan) beds. *Acta Anthropologica Sinica* 4:223–232. [Chinese 223–231; English 232]
- Zheng, S.-H., W.-Y. Wu, Y. Li, and G.-D. Wang. 1985. Late Cenozoic mammalian faunas of Guide and Gonghe Basins, Qinghai Province. *Vertebrata Palasiatica* 23:89–134. [Chinese 89–132; English 133–134]

Submitted August 15, 2012; revisions received June 1, 2013; accepted June 10, 2013.

Handling editor: Blaire Van Valkenburgh.